SCIENCE CHINA
Technological Sciences

•Article•

October 2023 Vol.66 No.10: 2786–2796
https://doi.org/10.1007/s11431-022-2310-5

# Tough adhesion and antifouling poly(vinyl alcohol) hydrogel coating on the arch wire for antibacterial adhesion

LI MingWen[1†], TANG Chen[2†], YU XiXi[1†], SHI XinLei[2], YU Hui[2], YIN HaiYan[2], YOU Min[2*], CHEN Qiang[2,3*] & DING Xi[1*]

[1] *Department of Stomatology, The First Affiliated Hospital of Wenzhou Medical University, Wenzhou 325000, China;*
[2] *Wenzhou Institute, University of Chinese Academy of Sciences, Wenzhou 325001, China;*
[3] *Oujiang Laboratory (Zhejiang Lab for Regenerative Medicine, Vision and Brain Health), Wenzhou 325000, China*

Received October 29, 2022; accepted January 3, 2023; published online August 10, 2023

The arch wire (AW) plays an important role in providing continuous force, aligning the teeth, and excellent dental arch stability for orthodontic treatment. However, the high friction performance of the AW surface can increase bacterial adhesion and colonization, leading to oral hygiene problems. Herein, a simple method is developed to modify the surface of the orthodontic wire with a poly(vinyl alcohol) (PVA) hydrogel coating, which can improve the lubricity and antibacterial adhesion of the AW and prevent the oral hygiene problems caused by itself. The PVA hydrogel coating can toughly adhere to the surface of the AW and remarkably reduce the friction performance of the AW, and then its friction coefficient in water can reach 0.005. Under the action of brushing and bending, the PVA hydrogel coating possesses superior ultralubrication and hardly affects the mechanical properties of the stainless-steel substrate. Moreover, the PVA hydrogel coating can significantly inhibit bacterial adhesion on the surface of the AW, thereby reducing bacterial colonization and maintaining oral hygiene while correcting the shape of the mouth and jaw. Therefore, the PVA hydrogel coating exhibits tough adhesion and good antibacterial adhesion while maintaining the mechanical properties of the AW, and it is a promising antifouling coating for improving the performance of the AW.

**orthodontic treatment, arch wire, hydrogel coating, tough adhesion, antifouling**

**Citation:** Li M W, Tang C, Yu X X, et al. Tough adhesion and antifouling poly(vinyl alcohol) hydrogel coating on the arch wire for antibacterial adhesion. Sci China Tech Sci, 2023, 66: 2786–2796, https://doi.org/10.1007/s11431-022-2310-5

## 1 Introduction

Malocclusion is mainly characterized by abnormal arch closure, misalignment of teeth, and malposition of the jaw [1,2]. According to the World Dental Federation, the incidence of malocclusion worldwide in people is as high as 56% [3]. Malocclusion mainly affects the development of teeth and maxillofacial, oral health, oral function and maxillofacial aesthetics, and even leads to serious psychological problems [4,5]. As the most widely used treatment in clinical practice, the fixed orthodontic treatment uses the orthodontic arch wire (AW) to exert force on the fixed appliance on the tooth, so that the dentition can be restored to the ideal state under the action of binding force [6]. The AW for orthodontic treatment should not only have high strength, low stiffness, and high plasticity, but also possess excellent friction performance, abrasion resistance, corrosion resistance, antibacterial performance, biocompatibility, aesthetic effect, and so on. Although stainless steel wire is one of the most widely used AW materials, there are some defects in the performance used in orthodontic clinics [7–9]. The friction force of AW during treatment will increase with the increasing surface roughness, which will reduce the ef-

†These authors contributed equally to this work.
*Corresponding authors (email: youmin@ucas.ac.cn; chenqiang@ucas.ac.cn; dingxi@wzhospital.cn)

ficiency of tooth movement and induce plaque accumulation, and even affect oral hygiene and health [10–12]. Due to the rapid development of biomedical engineering, various surface modification technologies recently have been developed to improve the surface performance of medical metal materials, especially the emerging hydrogel coating [13–19]. Therefore, the comprehensive properties of AW are greatly improved and the service life of AW is also prolonged.

To meet the clinical needs, varieties of materials have been used to modify metal arch wires, including polytetrafluoroethylene coating [20], diamond-like film [21], poly(chloro-para-xylylene) film [22], and $WS_2$ nanoparticles [23]. Although these coatings can partially improve the performance of the metal AW, some problems are still unavoidable such as low binding strength, low hardness, poor wear resistance, easy cracking, and terrible biocompatibility [24]. In addition, the coating on the surface of the AW is easily damaged by chewing force and saliva enzymes in the mouth, thus exposing the underlying metal. Due to being mechanically, chemically, and electrically compatible with living tissues [25,26], hydrogels are excellent coating materials for decorating the AW. Hydrogel-coated substrates can combine the advantages of hydrogels with the advantages of substrates, which displays stiffness, toughness, and strength while presenting lubricity, biocompatibility, and antibiofouling properties [27,28]. However, few of the reported hydrogel coatings can simultaneously meet the requirements of tough adhesion, antifouling, antibacterial adhesion, and biocompatibility [29]. As a typical hydrogel material, poly(vinyl alcohol) (PVA) hydrogel has unique advantages, including easy preparation, low cost, mass production, and good biocompatibility [30]. Fortunately, PVA hydrogel is also recognized as a hydrophilic, non-toxic, non-carcinogenic, non-biodegradable, and biocompatible material, which has been widely used in biomedical applications, such as contact lenses, soft joint replacements, wound dressings, hemodialysis membranes, and coatings for medical implants [31–33]. The PVA hydrogel coating not only shows tough adhesion to the substrate but also can be combined with a substrate with an arbitrary shape. In addition, PVA hydrogel is one of the biomaterials approved by the United States Food and Drug Administration (FDA) [24], which enables the PVA hydrogel coating to exhibit great potential in clinical application. Therefore, the PVA hydrogel coating combining tough adhesion and superior antibacterial adhesion may offer promising prospects in biomedical engineering.

In this work, a facile yet effective strategy, in which the antifouling PVA hydrogel coating is modified to the surface of the AW (PVA-AW), has been proposed to enhance the antibacterial adhesion of the AW. The PVA hydrogel coating is robustly anchored on the surface of AW due to the nanocrystalline domains of PVA itself [34,35]. Because of the large number of –OH groups and the chain density [36], the PVA hydrogel coating presents superior ultralubrication and antifouling properties, which can reduce bacterial adhesion and maintain oral hygiene. The antifouling PVA hydrogel coating robustly adhered to the surface of the AW by annealing at 100°C for 90 min. After being coated by the PVA hydrogel, the coefficient of friction (COF) of the AW was significantly reduced by nearly 0.005, indicating that the PVA hydrogel coating showed excellent ultralubrication. Furthermore, the PVA hydrogel coating on the surface of the AW could maintain excellent stability under different liquid environments, different bending angles, and brushing. Additionally, the bacterial survival state test indicated that the PVA-AW presented outstanding antibacterial adhesion using *Escherichia coli* (*E. coli*) and *Staphylococcus aureus* (*S. aureus*). Compared with bare-AW, the bacteria were difficult to proliferate on the PVA hydrogel coating, which was beneficial to improving oral hygiene and reducing complications such as enamel decalcification, dental caries, and periodontal disease [37,38]. Overall, the PVA hydrogel coating presented tough adhesion, outstanding antifouling, antibacterial adhesion, and biocompatibility. Therefore, this strategy circumvented costly and complicated procedures, demonstrating promising potential in orthodontic treatment.

## 2 Materials and methods

### 2.1 Materials

Poly(vinyl alcohol) (PVA1799, 99%), sodium chloride (NaCl), potassium chloride (KCl), urea, potassium thiocyanate (KSCN), potassium phosphate monobasic ($KH_2PO_4$), ammonium chloride ($NH_4Cl$), sodium bicarbonate ($NaHCO_3$), calcium chloride anhydrous ($CaCl_2$), sodium sulfate anhydrous ($Na_2SO_4$) were purchased from Shanghai Aladdin Biochemical Technology Co., Ltd. Luria Bertani Broth (miller) (LB) and tryptone soya broth (TSB) were purchased from Oxoid. *E. coli* and *S. aureus* were purchased from PerkinElmer, Inc., Waltham, MA. Phosphate buffer solution (PBS) was purchased from Beijing Solarbio Science & Technology Co., Ltd. Stainless steel wires (orthodontic arch wires, AW) (0.48 mm × 0.64 mm) were purchased from Heilongjiang LeiBo Co., Ltd. And 316 stainless steel sheets (SSSs, the thickness of SSSs is 0.1 mm) were purchased from the market. The bacterial live/dead staining kit for microscopy and quantitative assays was purchased from Invitrogen Co., Ltd. Centrifuge tubes, 12-well culture plates, and 1 μL inoculation loop were purchased from Wuxi NEST Biotechnology Co., Ltd. Deionized water was purified using CL-250L/H purification equipment (Suzhou, Chuanglian Co., Ltd.). All commercially obtained chemicals were used as received.

### 2.2 Preparation of PVA hydrogel coating

The antifouling PVA hydrogel coating was prepared on the surface of the stainless steel substrate. Briefly, 5 g PVA was firstly dissolved into 50 mL deionized water and continuously stirred at 600 r/min at 95°C for 2 h to form a 10% w/v PVA homogeneous solution. The cut SSSs (8 cm× 10 cm) and the silicone spacer molds were ultrasonically cleaned in ethanol and deionized water for 30 min at room temperature to remove the oil stains on their surfaces, respectively. To remove the surface oxide layer on the stainless steel, the cleaned substrates were treated with oxygen plasma (30 W at a pressure of 200 mTorr, Harrick Plasma PDC-001) for 5 min. Next, the 10% w/v PVA solution was poured onto stainless steel with a glass plate, and the stainless steel was surrounded by a 1 mm thick silicone spacer mold and a 0.1 mm thick polyethylene terephthalate (PET) film with a glass plate on the other side to form a reaction cell. After being fixed with clamps, the reaction cell was frozen at −20°C for 12 h to fabricate PVA hydrogel. After being removed from the reaction cell, the SSSs with PVA hydrogel (PVA-SSSs) were thawed at room temperature for 24 h. To achieve tough adhesion between PVA hydrogel and stainless steel, the dried PVA-SSSs were annealed at 100°C for 90 min in an oven. Finally, the obtained PVA-SSSs were immersed in water for 12 h to swell before further use. Moreover, the PVA-AW was also prepared as the above processes before testing.

### 2.3 Characterizations

The morphology of bare-AW and PVA-AW were observed by scanning electron microscopy (SEM, Phenom Pharos, Netherlands). Before SEM observation, the surfaces of bare-AW and PVA-AW were gold-plated. Fourier transform infrared (FT-IR) spectroscopy (BRUKER, Tensor II, Germany) was used to analyze the structure of wet PVA-SSSs soaked in five solutions (deionized water, 0.9% saline, artificial SAGF medium [39], 0.4% soda water, and tea water) for 12 h in the range of 4000–400 $cm^{-1}$ with a resolution of 4 $cm^{-1}$ (Table S1). Moreover, the structures of wet PVA-SSSs soaked in the above five solutions were performed by Raman spectroscopy (Renishaw Raman System, UK) with CW diode laser excitation at 532 nm. X-ray diffractometer (XRD, Bruker-AXS, Billerica, MA, US) within $2\theta$ range of 10°–90° was used to evaluate the crystalline phases of PVA-SSSs after soaking in the above five solutions. Differential scanning calorimetry (DSC, Series 2000) was used to evaluate the freezing resistance of PVA hydrogels after immersion in different solutions. The test was under a nitrogen gas flow rate of 50 mL/min and at a heating rate of 10°C/min from −50°C up to complete decomposition at 250°C. The weights of the samples were 5.10, 4.66, 5.90, 5.00, and 5.03 mg for dry PVA-water, dry PVA-SAGF, dry PVA-NaCl, dry PVA-$NaHCO_3$, and dry PVA-tea, respectively.

### 2.4 Mechanical measurement

The adhesion test of PVA hydrogel to SSS substrate was carried out on a Computerized Tensile Strength Testing Machine (KJ-1065A). The test samples were soaked in deionized water, 0.9% normal saline, artificial saliva, 0.4% soda water, and tea for 12 h. Next, a standard 90° peel test was performed on the PVA hydrogel samples attached to the SSS to measure the interfacial adhesion strength threshold $N$ ($J/m^2$). The PVA-SSSs soaked in different solutions were cut into rectangular shapes (100 mm × 10 mm), and a layer of double-sided tape was attached to the surface of the hydrogel samples as a substrate to prevent the influence of the tensile deformation of the hydrogel. The tensile rate was kept at 50 mm/min, the angle was 90°, the specimen was stretched at a speed of 50 mm/min to the set strain (100%), and then the strain was kept constant, and the stress change was monitored.

The adhesion energy ($J/m^2$) of the PVA hydrogel to the stainless steel interface was measured by a standard 90° peeling test. From a standard 90° peeling test, the adhesion energy $N$ was measured as follows: $W$ (m) was the width of the PVA hydrogel; $F$ (N) is the load; $N$ ($J/m^2$) was the adhesion energy [34].

$$N = 2F / W.$$

In addition, a thin and stiff layer of tape was attached to the surface of the PVA hydrogel sample as a backing to prevent it from extending along the surface of the sample in the peel direction.

### 2.5 Frictional test

A high-speed rheometer (DHR-2, TA Instruments, USA) with a 20 mm parallel plate geometry was used for the frictional tests. The PVA-SSSs were soaked in deionized water, 0.9% saline, artificial saliva, soda water, and tea water for 12 h. The PVA-SSSs were cut into disks of 10 mm in radius ($R$) and then glued onto the upper 20 mm stainless steel plate. In the steady sweep mode, the angular velocity ($\omega_a$) was $5\times10^{-4}$ – 30 rad/s. In the time sweep mode, $\omega_a$ was fixed at $10^{-3}$ rad/s, the measured time was 1000 s, and the torque ($T$) and instantaneous axial force ($N_a$) were detected. The experimental temperature was set at 25°C and the normal force was set to 1 N. The COF was calculated from $T$ and $N_a$, COF = $4T/3RN_a$ [40], and every frictional test was repeated three times.

### 2.6 Antibacterial adhesion tests

The antibacterial adhesion of PVA-SSS and PVA-AW sam-

ples were evaluated with *E. coli* and *S. aureus*. *E. coli* were incubated on an LB agar medium overnight at 37°C. Then, the single bacterial colony was inoculated into LB liquid medium and cultured overnight with continuous shaking. The culture was diluted with LB medium to an OD value of 0.1 after 24 h. The PVA-SSSs, bare-AWs, and PVA-AWs samples were divided into five groups, namely the untreated group, the bending group at 30°, the bending at 60°, the bending at 90° (both bending 1000 times), and the brushing group. In the brushing group, the PVA-SSSs or PVA-AWs were dipped in an electric toothbrush with an appropriate amount of toothpaste to simulate the normal brushing environment. The five groups of PVA-SSSs were cut into a specific size (1 cm × 1 cm), exposed to UV light for 30 min for pre-sterilization, and then placed in 12-well plates, respectively. Then, 2 mL of *E. coli* solution (0.1 OD) was added to each well, and incubated at 37°C for different incubation time, 1, 3, and 7 d, respectively. In addition, the blank polystyrene (PS) plate or the bare-AW was used as a control group, and 2 mL of *E. coli* solution (0.1 OD) was also added to the blank PS plate or the bare-AW, and incubated at 37°C for different incubation time, 1, 3, and 7 d, respectively. Using the same method as above, *S. aureus* was incubated on a TSB agar medium overnight at 37°C. Then, single colonies were inoculated in TSB liquid medium and cultured overnight with continuous shaking. After 24 h, the cultures were diluted with TSB broth to an OD of 0.1. Repeat the above experimental procedure with *S. aureus* (0.1 OD). To compare the number of bacteria, the PVA hydrogels were stripped from the substrates and washed three times with PBS, using the live/dead backlight activity kit to stain the hydrogels. The morphology of live/dead bacteria on the surface of the hydrogel was observed and counted using an Axio Observer A1 fluorescence microscope (Carl Zeiss, Germany).

## 3 Results and discussion

### 3.1 Design and preparation

The AW is an important piece of equipment in the process of orthodontic treatment, which can constrain the teeth and transmit the orthodontic force to guide the tooth movement, thereby regulating the three-dimensional movement of the teeth to achieve orthodontic treatment. However, the AW is easy to be embedded in food debris to induce bacterial growth because of the complex oral environment. Therefore, the antifouling PVA hydrogel in this work was used as a coating material to coat the surface of the AW for reducing friction and preventing bacterial adhesion on the surface of the AW toward maintaining oral hygiene (Figure 1). The PVA hydrogel coating was modified onto the surface of the AW, and then the PVA hydrogel coating with AW was annealed to form nanocrystalline structures with hydrogen bonds for obtaining a remarkable tough adhesion between PVA hydrogel and AW (Figure 1(a)). Moreover, the PVA hydrogel coating significantly reduced the COF of the AW. Due to the abundance hydroxyl group, the PVA hydrogel coating on the AW presented remarkable steric exclusion effect and surface hydration layer that contributed to antifouling performance and resisted the adhesion of bacteria, thus achieving the effect of antibacterial adhesion (Figure 1(b)). Therefore, the PVA hydrogel coating on the surface of the AW could significantly improve its antibacterial adhesion performance and maintain oral hygiene while orthodontics.

### 3.2 Characterization

To characterize the PVA hydrogel coating on the surface of the AW, SEM was used to investigate the surface morphology of PVA-AW. As shown in Figure 2(a) and (b), the surface texture of PVA-AW was much finer than that of bare-AW, which was conducive to the antibacterial adhesion of PVA hydrogel coating. The cross-section images of bare-AW and PVA-AW presented that the size of AW was 0.48 mm × 0.64 mm (Figure 2(c)). As shown in Figure 2(d), the PVA hydrogel coating could be clearly observed on the surface of the AW. And the thickness of PVA hydrogel coating was about 15 μm. To further demonstrate the PVA hydrogel coating on the AW surface, the SEM mappings of PVA-AW were performed (Figure 2(e)). The distributions of carbon (C) and oxygen (O) elements were delimited from that of iron (Fe) elements, and the distributions of C and O were hardly distributed in the Fe. Furthermore, the PVA-AW was dyed with green dye, and the fluorescence microscope image indicated that the thickness of the PVA hydrogel coating was approximately 16 μm (Figure 2(f)), which was in agreement with the results obtained from SEM.

Besides, FT-IR spectroscopy was also used to test the state of PVA hydrogel under normal oral liquid environments (deionized water, 0.9% normal saline, artificial saliva, 0.4% soda water, and tea). As shown in Figure 3(a), the obvious infrared absorbance characteristic peaks at 3300 $cm^{-1}$ were assigned to the O–H stretching [41]. The main absorption bands around 1632, 1421, and 1091 $cm^{-1}$ were assigned to the C=O stretching, the $–CH_2–$ stretching, and the C–O stretching vibration, respectively [42–44]. The FT-IR spectra of the different solutions were essentially the same, indicating that the structure of PVA hydrogel coating could maintain excellent stability under normal oral liquid environments. Moreover, the Raman spectra were used to investigate the state of PVA hydrogel after immersing it in the above solution for 12 h. The bands at 2900, 1441, and 1125 $cm^{-1}$ were assigned to the C–H stretching [45], the $–CH_2–$ stretching, and the C–O stretching [46] (Figure 3(b)). Besides, the bands at 912 and 847 $cm^{-1}$ were assigned to the

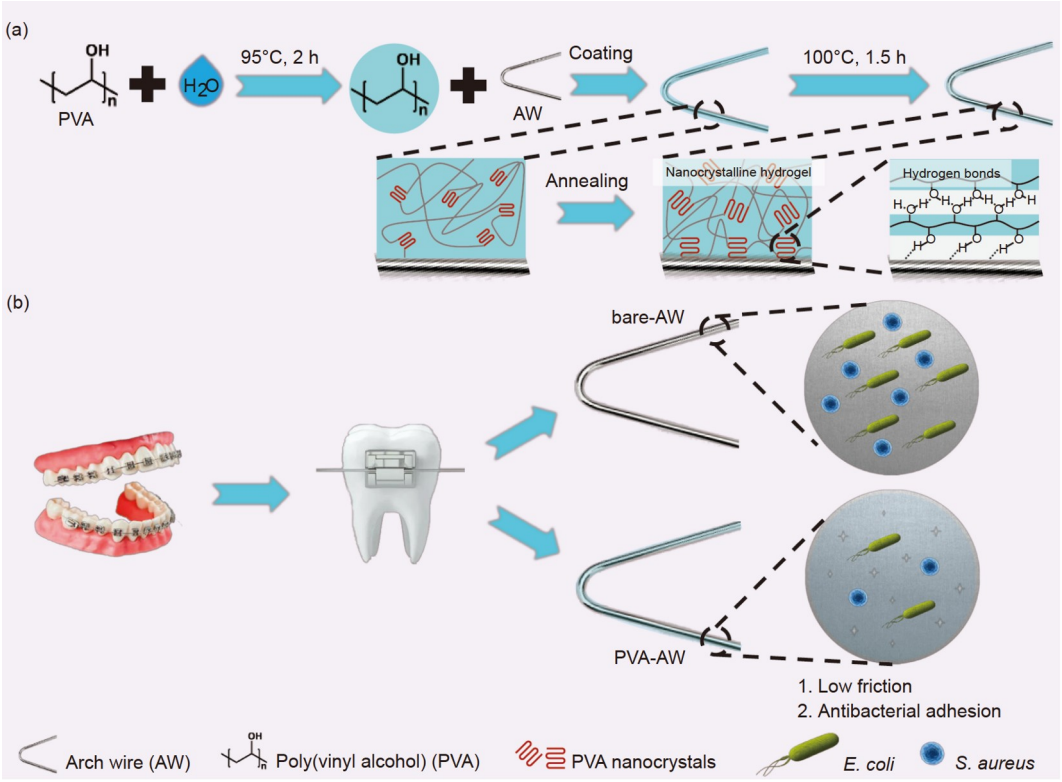


**Figure 1** (Color online) Schematic illustration of the tough adhesion and antifouling PVA hydrogel coating on the surface of the AW for antibacterial adhesion. (a) Schematic representation of the formation of PVA-AW and the tough adhesion of PVA hydrogel to AW by anchoring ordered nanocrystalline structures on the AW with hydrogen bonds. (b) Schematic diagram showing the design of a dental appliance with low friction and antibacterial adhesion.

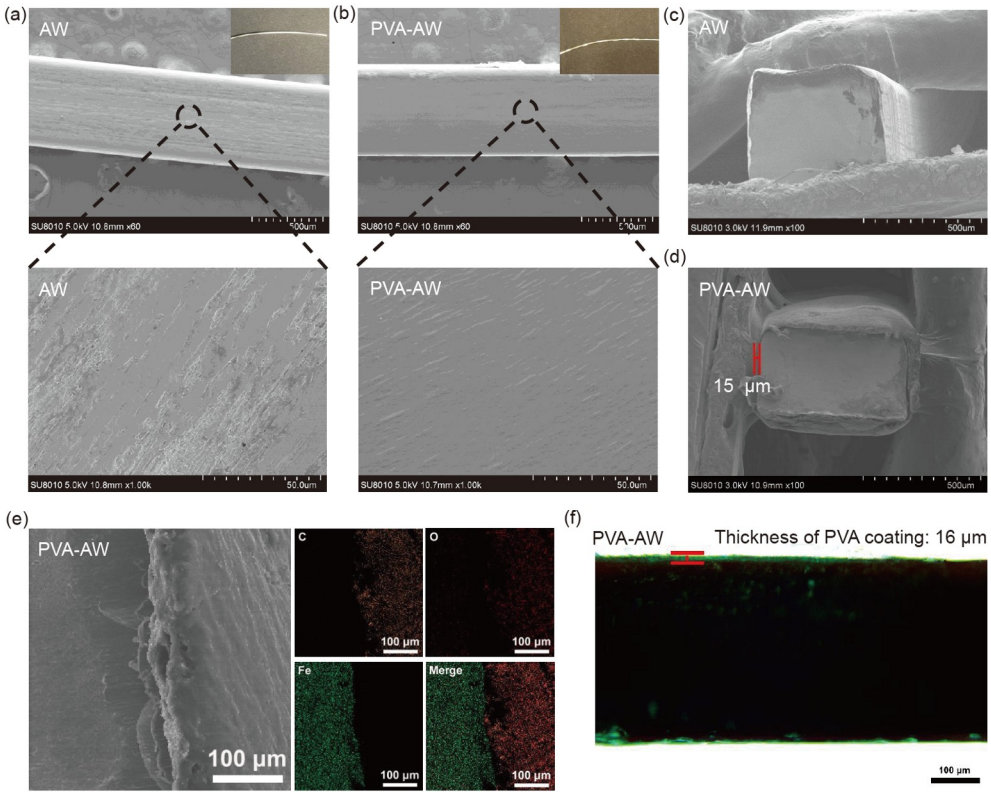


**Figure 2** (Color online) Preparation and characterization of the PVA hydrogel coating on the surface of the AW. SEM images of (a) bare-AW and (b) PVA-AW (scale bar: 500 μm and 50 μm). Insets of (a) and (b) were the photographs of bare-AW and PVA-AW. SEM images of the cross-section of (c) bare-AW and (d) PVA-AW (scale bar: 500 μm). (e) SEM and corresponding elemental mapping images of PVA-AW. (f) Photograph of PVA-AW dyed with green dye.

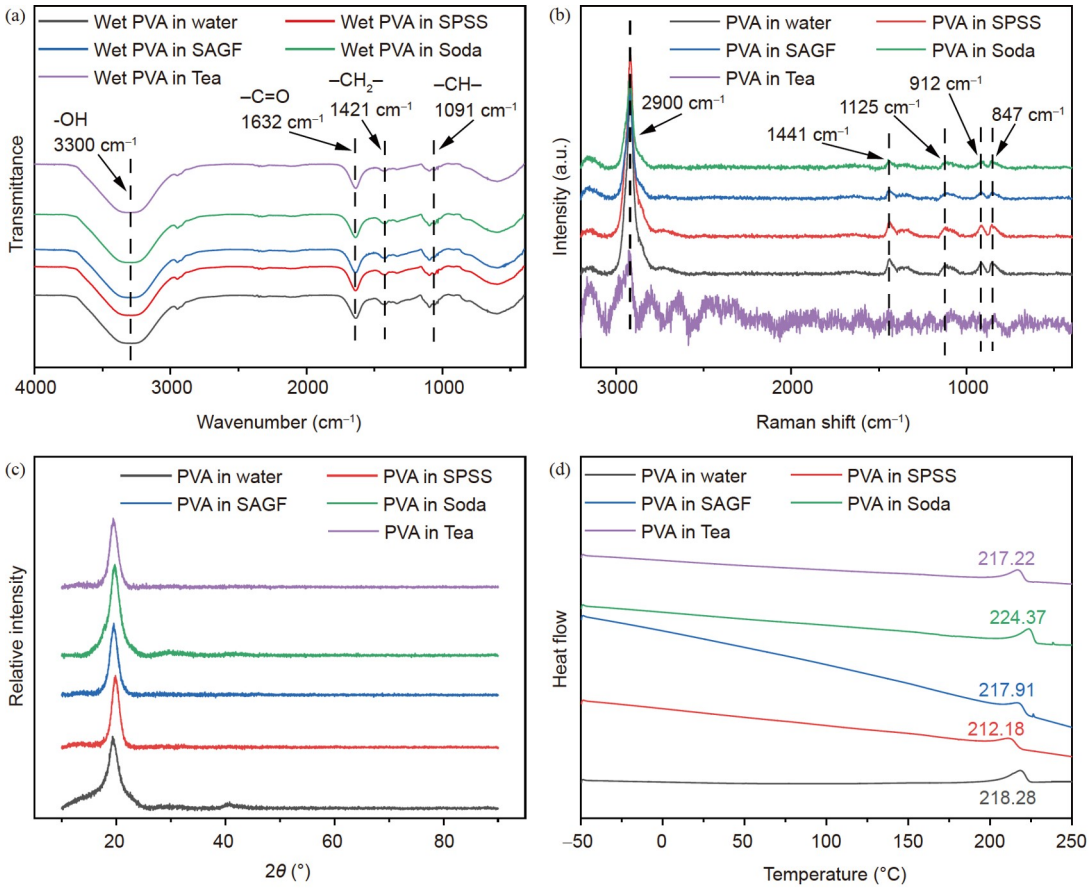


**Figure 3** Characterization of the wet PVA films incubated with deionized water, 0.9% saline, artificial saliva, 0.4% soda water, and tea for 12 h. (a) FTIR spectra, (b) Raman spectra, (c) XRD patterns, and (d) DSC curves of the wet PVA films treated with the above solutions.

C–C stretching [46]. No significant shift occurred in all the bands of Raman spectra above, indicating that the treatment of different solutions did not change the structure of PVA hydrogel coating. The XRD patterns of PVA hydrogels soaked in the above solutions suggested that the characteristic peak of the PVA crystalline phase was near 19.28° (Figure 3(c)), attributing to the intermolecular hydrogen bond between PVA chains [47]. Furthermore, the DSC heating curves of PVA hydrogels soaked with different solutions showed a peak endotherm ranging from 212.18°C to 224.37°C (Figure 3(d)), demonstrating that the crystallinity of PVA hydrogels maintained superior stability at various solutions. Consequently, the PVA hydrogels were successfully modified on AW and maintained good stability.

### 3.3 Tough adhesion

To investigate the adhesion of PVA hydrogel coating, the interfacial toughness of PVA hydrogels was characterized through the 90° peeling test with a stiff backing on the PVA hydrogels (Figure 4(a) and (b)). In the test, the PVA hydrogel showed an adhesion energy near 1000 N/m and showed very close adhesion energies after being immersed in different liquids (deionized water, 0.9% saline, artificial saliva, soda water, and tea) for 12 h (Figure 4(c) and (d)). The nanocrystalline domains and unique chemical structure of PVA hydrogel coating enable it to be robustly anchored on the surface of the metal substrates [48,49]. After being soaked with different solutions, all PVA hydrogels showed adhesion energies of approximately 1000 N/m, demonstrating that the PVA hydrogel coating could still robustly adhere to the surface of SSSs in the complex liquid environment simulating the mouth. As shown in Figure 4(e), the adhesion energies of PVA hydrogel were similar when the PVA hydrogels were bent at different angles (30°, 60°, 90°) for 1000 times and then immersed in deionized water for 12 h. After bending at different angles, the PVA-SSSs were immersed in different solutions (Figure 4(f)). And all the adhesion energies of PVA hydrogels were similar, suggesting that the PVA hydrogel coating could still strongly adhere to the surface of SSS during the mechanical occlusal movement of the mouth. Importantly, the PVA hydrogel showed very close adhesion energies as the PVA hydrogels were brushed by a toothbrush for 1 min and then immersed in deionized water for 12 h (Figure 4(g)). Moreover, the adhesion energies of PVA hydrogels were nearly 1000 N/m when the PVA-SSSs were brushed for 1 min and then immersed in different solutions (Figure 4(h)). It indicated that the slight mechanical

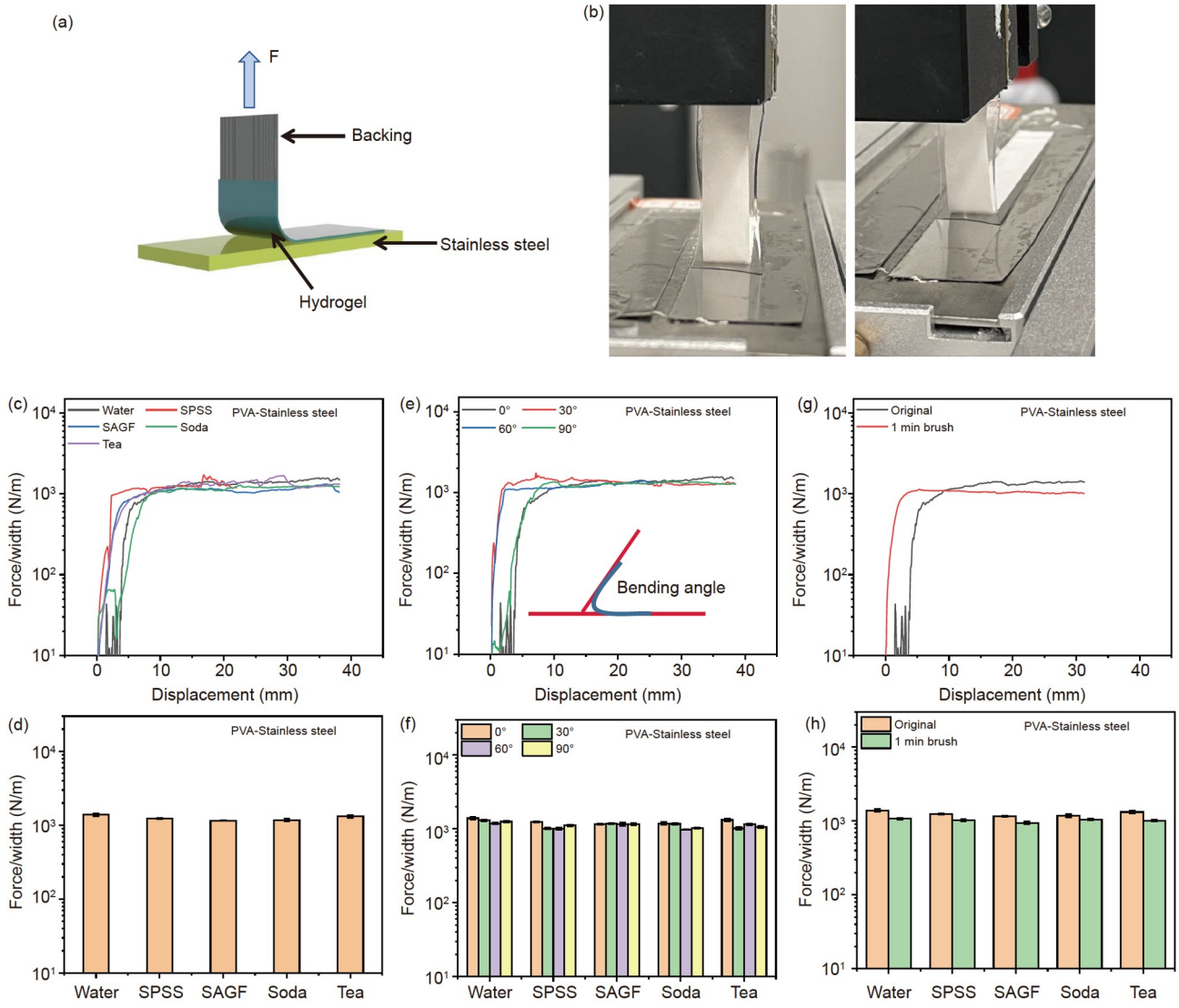


**Figure 4** Adhesion properties of PVA hydrogel coating through 90° peeling test. (a) Schematic illustration of PVA hydrogel 90° peeling test. (b) Photographs of the interface in PVA hydrogel 90° peeling test. (c) Force/width versus displacement curves of PVA hydrogels incubated with deionized water, 0.9% saline, artificial saliva, 0.4% soda water, and tea for 12 h before the 90° peel test. (d) The interfacial toughness of PVA hydrogels incubated with the above solutions. (e) Force/width versus displacement curves of PVA hydrogels incubated with deionized water for 12 h treated with different bending angles 1000 times before the 90° peel test. Inset of (e) was a simulation of the PVA-SSS bending method. (f) The interfacial toughness of PVA hydrogels was incubated with the above solutions for 12 h after treating them with different bending angles 1000 times. (g) Force/width versus displacement curves of PVA hydrogels adhered to stainless steel, following incubated with deionized water and treated with a toothbrush for 1 min. (h) The interfacial toughness of PVA hydrogels was incubated with the above solutions after treating them with a toothbrush for 1 min. All of the above data are presented as mean ± SD ($n$ = 3).

damage in the mouth had little influence on the adhesion of the PVA hydrogel coating before the destruction of the PVA hydrogel coating to the exposure of the AW. In conclusion, the PVA hydrogel coating on the surface of the AW maintained outstanding stability under various human oral conditions, including different liquid environments, different bending angles, and brushing.

### 3.4 Friction testing

The COF was the key index to evaluate the lubricity of PVA hydrogel coating. Hence, the friction properties of PVA hydrogels were investigated in terms of different normal forces, frequencies, the thickness of the PVA hydrogel coating, and the oral fluid environment. Attributing to the small size of the square AW, the stainless-steel sheets with the same material were used to replace the AW to complete relevant tests in this work. The COF of the antifouling PVA hydrogel coating was carried out with disk samples against a stainless steel surface. At the frequency of 0.5 Hz, the COF of PVA-SSS in water decreased as the applied normal force increased ranging from 0.5 to 4 N (Figure 5(b)). Moreover, the COF of the antifouling PVA hydrogel coating was 0.016 at 0.5 N, which was more than twice compared with other normal forces. The

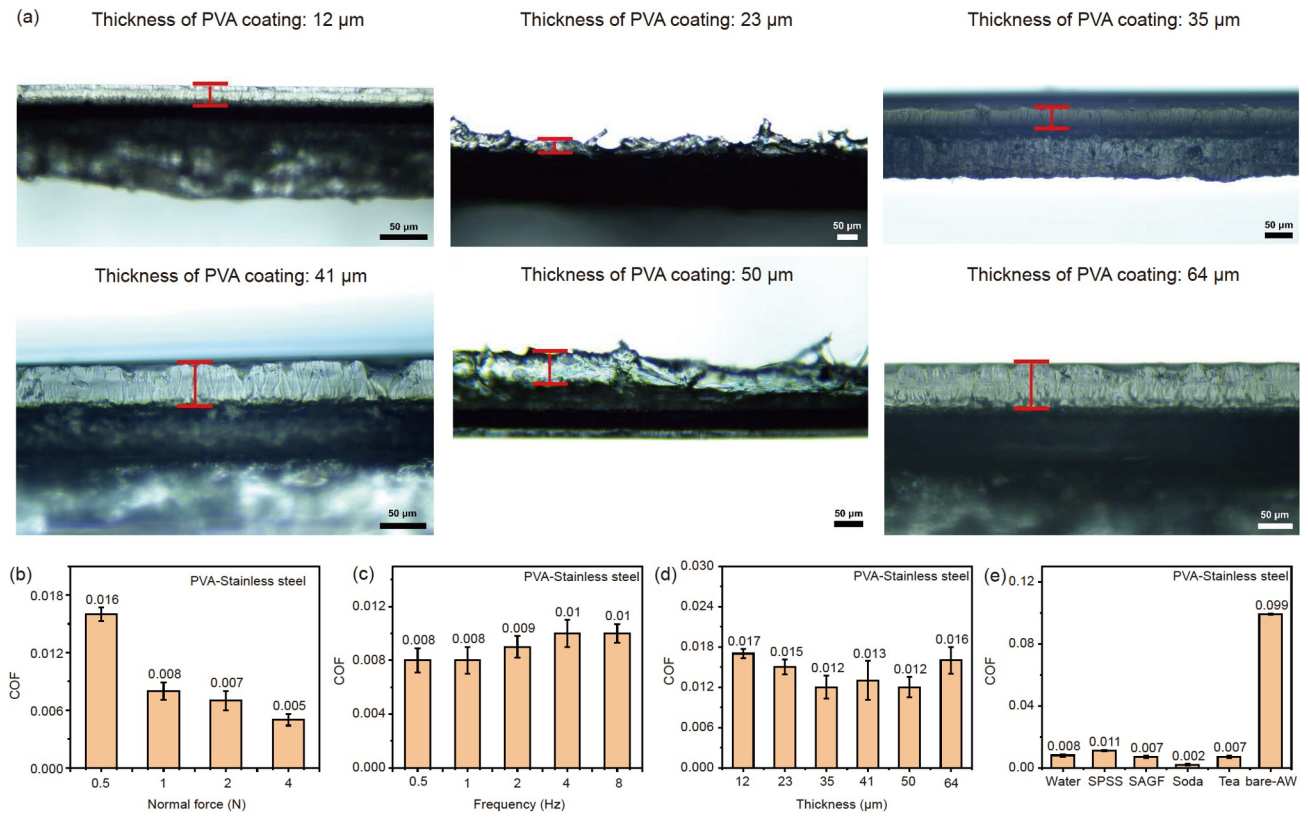


**Figure 5** (Color online) The friction performance of PVA hydrogels coating. (a) Photographs of different thicknesses of PVA hydrogels coating on the SSSs. (b) The frictional performance of PVA hydrogels under different normal forces at 0.5 Hz. (c) The frictional performance of PVA hydrogels under different frequencies with 1 N normal force. (d) The frictional performance of different thicknesses of PVA hydrogels coating incubated with deionized water for 12 h under 1 N normal force and 0.5 Hz. (e) The frictional performance of PVA hydrogels was incubated with deionized water, 0.9% saline, artificial saliva, 0.4% soda water, and tea for 12 h under 1 N normal force and 0.5 Hz.

COFs were below 0.01 and closed in value when the applied normal force was in the range of 1 to 4 N, and the COF of PVA hydrogel in water was 0.005 when the applied normal force was 4 N. Thus, 1 N acted as the optimal normal force in following experiments. Furthermore, the COF of PVA hydrogel in water slightly increased with the increase of applied frequency ranging from 0.5 to 8 Hz with 1 N normal force, and the values of COFs were near 0.01 and closed (Figure 5(c)). Hence, the optimal frequency was set to 1 Hz in the following experiments. To investigate the effect of coating thickness on its lubrication, the different thicknesses of the PVA hydrogel coating were prepared ranging from 12 to 64 μm (Figure 5(a)). Figure 5(d) showed that the COFs of PVA hydrogel in water fluctuated between 0.012 and 0.017 under optimized conditions, demonstrating that the thickness of hydrogel had little effect on the COF, lubrication, and antibacterial adhesion properties. As shown in Figure 5(e), the COF of bare-AW was 0.099. And the COFs of PVA-SSSs in different solutions (deionized water, 0.9% saline, artificial saliva, soda water, and tea) were near 0.007, which was significantly less than that of bare-AW. These results demonstrated that the antifouling PVA hydrogel coating significantly reduced the COF of the AW, presented outstanding ultralubrication, and maintained the stability of the AW in the oral liquid environment.

### 3.5 Antibacterial adhesion

The antibacterial adhesion performance of PVA hydrogels coating was evaluated by the bacterial survival state test using *E. coli* and *S. aureus* within 7 d. Firstly, PVA-SSSs were used to evaluate the antibacterial adhesion of PVA hydrogel coating. The PS plate was used as the control, and the PVA-SSSs that had been bent at different angles (0, 30°, 60°, 90°) and brushed for 1 min acted as the experimental groups. Compared with the PS plate, a few live and dead *E. coli* could be observed within 1, 3, and 7 d (Figure S1(a)), indicating that the *E. coli* could hardly adhere to the PVA hydrogel interfaces during the test. The number of *E. coli* on the surface of hydrogels undergone bending and brushing was much higher than that of the original PVA hydrogel (Figure S1). In addition, quantitative calculations of live/dead bacterial density were evaluated using ImageJ software

according to fluorescence microscopy images. As shown in Figure S1(b) and (c), the densities of live and dead *E. coli* adhering to the PVA hydrogel increased slightly within 7 d, suggesting that it was difficult for *E. coli* to adhere and proliferate on the surface of PVA hydrogels in the PVA-SSSs. During the decay period, the limited nutrients and the accumulation of various toxic metabolites near the bacteria could affect the growth of the bacteria and eventually lead to death of the bacteria. Therefore, the dead bacteria on the surface of PVA hydrogel were the normal death of bacteria. Meanwhile, the *S. aureus* was also tested as same as the *E. coli*, and the results demonstrated that the *S. aureus* was difficult to adhesion and proliferate on the surface of PVA hydrogels (Figure S2). Due to the antifouling performance and lower COF of PVA hydrogels, the SSSs with the PVA hydrogel coating displayed remarkable antibacterial adhesion properties.

Besides, *E. coli* and *S. aureus* were also used to evaluate the antibacterial adhesion of bare-AW and PVA-AW samples. The LIVE/DEAD cell viability assays were used to explore the antibacterial adhesion of the PVA hydrogel coating. Fluorescence microscope images revealed a general trend of adhesive bacterial density and bacterial distribution on bare-AW and PVA-AW within 7 d (Figures 6 and S3). As shown in Figures 6(a) and S3, the *E. coli* was observed to significantly adhere and aggregate on bare-AW. The bacterial adhesion on PVA-AW decreased dramatically after bending and brushing compared with bare-AW, indicating that PVA-AW had antibacterial adhesion and colony-suppressing properties. On the other hand, a small amount of bacterial proliferation was observed on PVA-AW without the disruption of the PVA hydrogel coating over time, which was probably attributed to the lubricity and antibacterial adhesion of the PVA hydrogel coating. A large of adherent bacteria ($9.3 \times 10^5$ cm$^{-2}$) on bare-AW were alive, and all the PVA-AW samples had significantly lower bacterial density than that of the bare-AW samples (Figure 6(b) and (c)). The statistical results of the live/dead bacteria demonstrated that the PVA hydrogel coating endowed the stainless-steel AW with outstanding antibacterial adhesion, which was probably due to the combination of PVA's lubricity and antifouling performance. Furthermore, *S. aureus* was also tested as same as the *E. coli*. As shown in Figures 7 and S4, *S. aureus* was also difficult to adhesion and proliferate on the surface of PVA hydrogels coating, which was in agreement with those from *E. coli*. Consequently, the AW with the PVA hydrogel coating showed superior antibacterial adhesion attributed to the low COF and antifouling performance of PVA hydrogels.

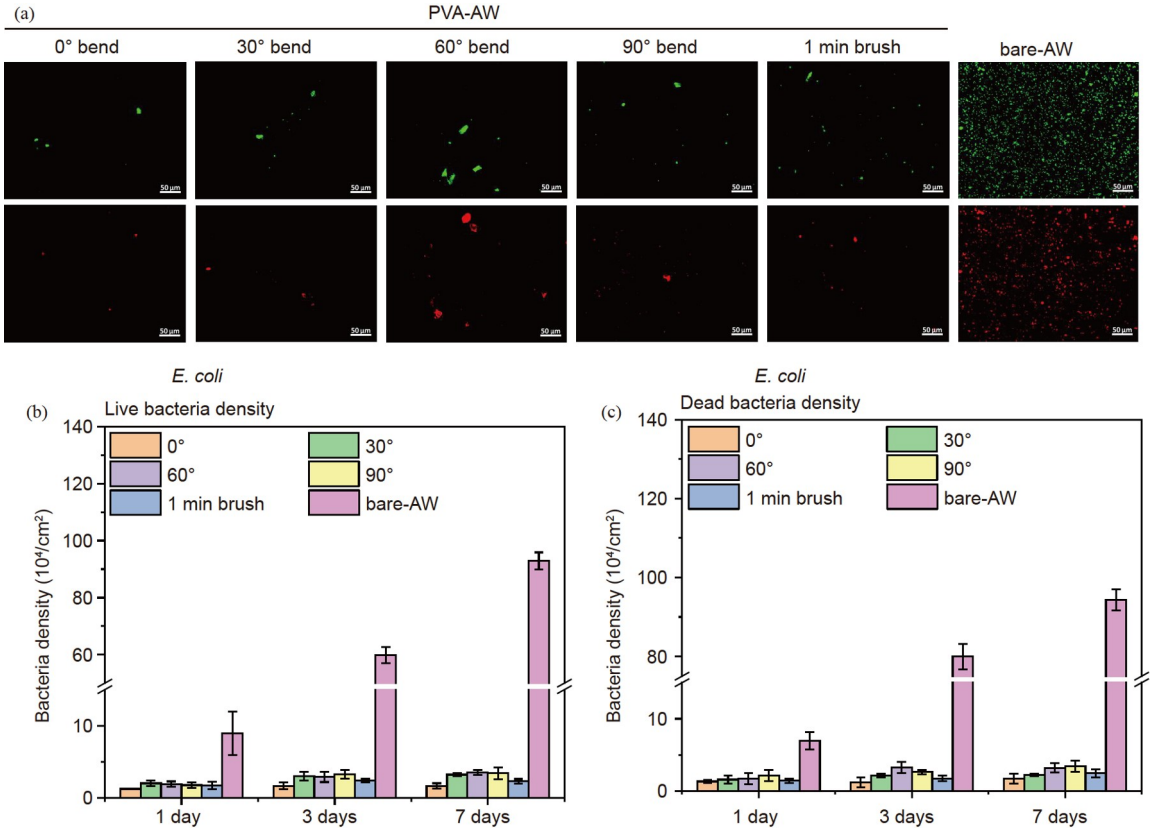


**Figure 6** Antibacterial adhesion of PVA-AW against *E. coli*. (a) Fluorescence microscope images of *E. coli* live/dead staining (green fluorescence: calcein-AM indicates live bacteria; red fluorescence: propidium iodide indicates dead bacteria) cultured for 7 days on the surface of bare-AW and differently treated PVA-AW. Scale bars: 50 μm. (b) The bacteria density of live *E. coli* on the surface of bare-AW and differently treated PVA-AW after different incubation time. (c) The bacteria density of dead *E. coli* on the surface of bare-AW and differently treated PVA-AW after different incubation time.

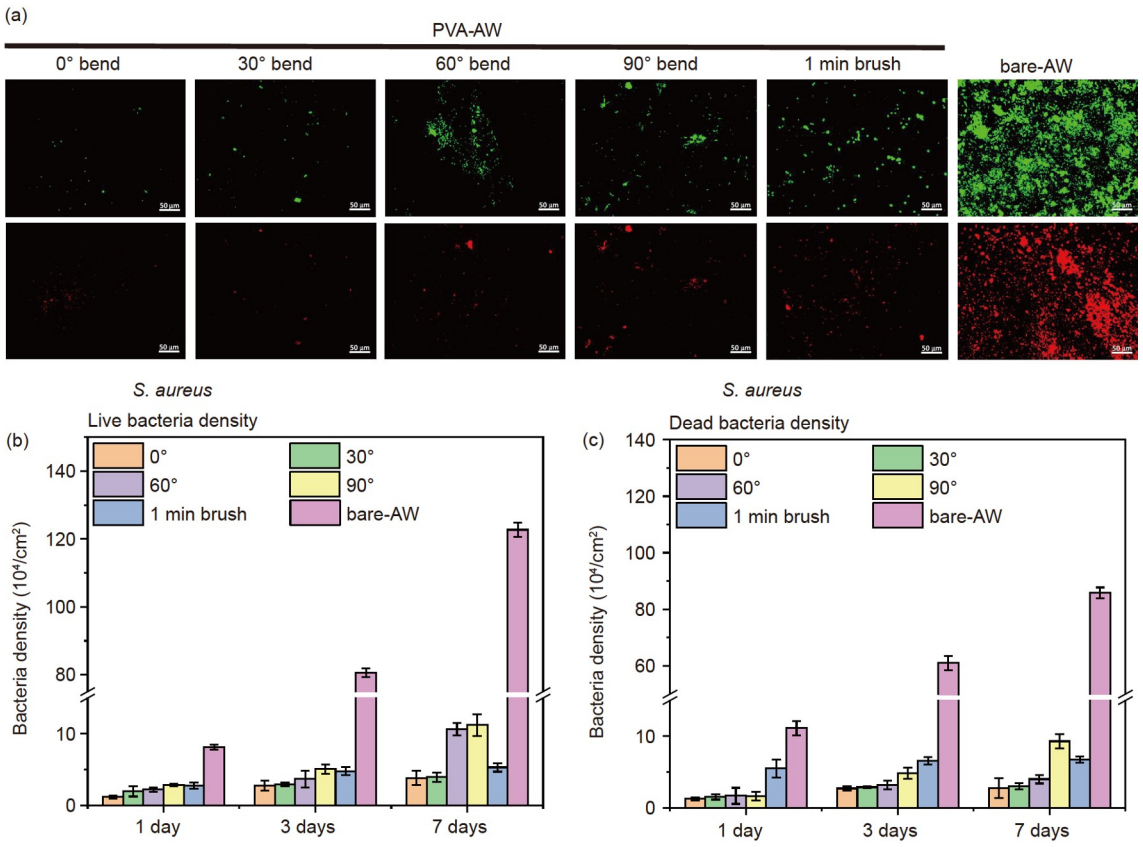


**Figure 7** Antibacterial adhesion of PVA-AW against *S. aureus*. (a) Fluorescence microscope images of *S. aureus* live/dead staining (green fluorescence: calcein-AM indicates live bacteria; red fluorescence: propidium iodide indicates dead bacteria) cultured for 7 d on the surface of bare-AW and differently treated PVA-AW. Scale bars: 50 μm. (b) The bacteria density of live *S. aureus* on the surface of bare-AW and differently treated PVA-AW after different incubation time. (c) The bacteria density of dead *S. aureus* on the surface of bare-AW and differently treated PVA-AW after different incubation time.

## 4 Conclusions

In summary, a tough adhesion and antifouling PVA hydrogel coating was successfully modified on the surface of the AW to enhance its antibacterial adhesion performance. The PVA hydrogel coating toughly adhered to the surface of the AW under various physical actions including bending and brushing, owing to its nanocrystalline domains, and remained stable in different oral liquid environments. The friction tests showed that the PVA hydrogel coating presented excellent ultralubrication and had a lower coefficient of friction compared with bare-AW. And the friction coefficient of the AW coated by PVA hydrogel coating could even reach 0.005, which could effectively reduce the friction between the AW and the bracket and improve the effectiveness of the orthodontic effect. Furthermore, the antibacterial adhesion tests demonstrated that *E. coli* and *S. aureus* were difficult to adhere to PVA-AW, resulting in the long-term antibacterial adhesion effect of PVA-AW. Taken together, the tough adhesion and antifouling PVA hydrogel is a promising coating material for the orthodontic wire to manage oral hygiene, which presents great potential in clinical dental treatment.

*This work was supported by Excellent Youth Fund Project of Henan Natural Science Foundation (Grant No. 202300410166), the National Natural Science Foundation of China (Grant No. 22202051), the Major Project of WIUCAS (Grant Nos. WIUCASQD2021004 and WIUCASQD2021035), the Project of Wenzhou Key Lab (Grant No. 2021HZSY0069), and the Science Foundation of Oujiang Laboratory (Grant No. OJQDSP2022018).*

### Supporting Information

The supporting information is available online at tech.scichina.com and link.springer.com. The supporting materials are published as submitted, without typesetting or editing. The responsibility for scientific accuracy and content remains entirely with the authors.

1 Alhammadi M S, Halboub E, Fayed M S, et al. Global distribution of malocclusion traits: A systematic review. Dental Press J Orthod, 2018, 23: 40e1–40e10
2 Magalhães I B, Pereira L J, Marques L S, et al. The influence of malocclusion on masticatory performance. Angle Orthod, 2010, 80: 981–987
3 Lombardo G, Vena F, Negri P, et al. Worldwide prevalence of malocclusion in the different stages of dentition: A systematic review and meta-analysis. Eur J Paediatr Dent, 2020, 21: 115–122
4 Kragt L, Dhamo B, Wolvius E B, et al. The impact of malocclusions on oral health-related quality of life in children—A systematic review and meta-analysis. Clin Oral Invest, 2016, 20: 1881–1894
5 Martins-Júnior P A, Marques L S, Ramos-Jorge M L. Malocclusion: Social, functional and emotional influence on children. J Clin Pediatr

Dent, 2012, 37: 103–108
6 Nikolai R J. Orthodontic wire: A continuing evolution. Semin Orthod, 1997, 3: 157–165
7 Antezack A, Monnet-corti V. Hygiène orale et parodontale chez les patients porteurs de dispositifs orthodontiques. Orthod Fr, 2018, 89: 181–190
8 Artun J, Brobakken B O. Prevalence of carious white spots after orthodontic treatment with multibonded appliances. Eur J Orthod, 1986, 8: 229–234
9 Gorelick L, Geiger A M, Gwinnett A J. Incidence of white spot formation after bonding and banding. Am J Orthod, 1982, 81: 93–98
10 An J S, Kim K, Cho S, et al. Compositional differences in multi-species biofilms formed on various orthodontic adhesives. Eur J Orthod, 2017, 39: 528–533
11 Ghasemi T, Arash V, Rabiee S M, et al. Antimicrobial effect, frictional resistance, and surface roughness of stainless steel orthodontic brackets coated with nanofilms of silver and titanium oxide: A preliminary study. Microsc Res Tech, 2017, 80: 599–607
12 Muller L K, Jungbauer G, Jungbauer R, et al. Biofilm and orthodontic therapy. Monogr Oral Sci, 2021, 29: 201–213
13 Borzabadi-Farahani A, Borzabadi E, Lynch E. Nanoparticles in orthodontics, a review of antimicrobial and anti-caries applications. Acta Odontologica Scandinavica, 2014, 72: 413–417
14 Huang S Y, Huang J J, Kang T, et al. Coating NiTi archwires with diamond-like carbon films: Reducing fluoride-induced corrosion and improving frictional properties. J Mater Sci-Mater Med, 2013, 24: 2287–2292
15 Kobayashi S, Ohgoe Y, Ozeki K, et al. Dissolution effect and cytotoxicity of diamond-like carbon coatings on orthodontic archwires. J Mater Sci-Mater Med, 2007, 18: 2263–2268
16 Peng L, Chang L, Liu X, et al. Antibacterial property of a polyethylene glycol-grafted dental material. ACS Appl Mater Interfaces, 2017, 9: 17688–17692
17 Peng L, Chang L, Si M, et al. Hydrogel-coated dental device with adhesion-inhibiting and colony-suppressing properties. ACS Appl Mater Interfaces, 2020, 12: 9718–9725
18 Ryu H S, Bae I H, Lee K G, et al. Antibacterial effect of silver-platinum coating for orthodontic appliances. Angle Orthod, 2012, 82: 151–157
19 Wu X, Liu S, Chen K, et al. 3D printed chitosan-gelatine hydrogel coating on titanium alloy surface as biological fixation interface of artificial joint prosthesis. Int J Biol Macromolecules, 2021, 182: 669–679
20 Husmann P, Bourauel C, Wessinger M, et al. The frictional behavior of coated guiding archwires. J Orofacial Orthop Fortschritte der Kieferorthopädie, 2002, 63: 199–211
21 Muguruma T, Iijima M, Brantley W A, et al. Effects of a diamond-like carbon coating on the frictional properties of orthodontic wires. Angle Orthod, 2011, 81: 141–148
22 Zufall S W, Kusy R P. Sliding mechanics of coated composite wires and the development of an engineering model for binding. Angle Orthod, 2000, 70: 34–47
23 Redlich M, Katz A, Rapoport L, et al. Improved orthodontic stainless steel wires coated with inorganic fullerene-like nanoparticles of $WS_2$ impregnated in electroless nickel-phosphorous film. Dent Mater, 2008, 24: 1640–1646
24 Yuk H, Wu J, Zhao X. Hydrogel interfaces for merging humans and machines. Nat Rev Mater, 2022, 7: 935–952
25 Chen H, Yang F, Chen Q, et al. A novel design of multi-mechanoresponsive and mechanically strong hydrogels. Adv Mater, 2017, 29: 1606900
26 Tang Z, He H, Zhu L, et al. A general protein unfolding-chemical coupling strategy for pure protein hydrogels with mechanically strong and multifunctional properties. Adv Sci, 2022, 9: 2102557
27 Liu J, Qu S, Suo Z, et al. Functional hydrogel coatings. Natl Sci Rev, 2021, 8: nwaa254
28 Fu M, Liang Y, Lv X, et al. Recent advances in hydrogel-based anti-infective coatings. J Mater Sci Tech, 2021, 85: 169–183
29 Riga E K, Rühe J, Lienkamp K. Non-delaminating polymer hydrogel coatings via C,H-insertion crosslinking (CHic)—A case study of poly (oxanorbornenes). Macromol Chem Phys, 2018, 219: 1800397
30 Singh B, Pal L. Radiation crosslinking polymerization of sterculia polysaccharide-PVA-PVP for making hydrogel wound dressings. Int J Biol Macromolecules, 2011, 48: 501–510
31 Mansur H S, Costa H S. Nanostructured poly(vinyl alcohol)/bioactive glass and poly(vinyl alcohol)/chitosan/bioactive glass hybrid scaffolds for biomedical applications. Chem Eng J, 2008, 137: 72–83
32 Alves M H, Jensen B E B, Smith A A A, et al. Poly(vinyl alcohol) physical hydrogels: New vista on a long serving biomaterial. Macromol Biosci, 2011, 11: 1293–1313
33 Baker M I, Walsh S P, Schwartz Z, et al. A review of polyvinyl alcohol and its uses in cartilage and orthopedic applications. J Biomed Mater Res B Appl BioMater, 2012, 100B: 1451–1457
34 Liu J, Lin S, Liu X, et al. Fatigue-resistant adhesion of hydrogels. Nat Commun, 2020, 11: 1071
35 Lin S, Liu X, Liu J, et al. Anti-fatigue-fracture hydrogels. Sci Adv, 2019, 5: eaau8528
36 Ben Halima N. Poly(vinyl alcohol): Review of its promising applications and insights into biodegradation. RSC Adv, 2016, 6: 39823–39832
37 Li Q, Liu J, Xu Y, et al. Fast cross-linked hydrogel as a green light-activated photocatalyst for localized biofilm disruption and brush-free tooth whitening. ACS Appl Mater Interfaces, 2022, 14: 28427–28438
38 Gkantidis N, Christou P, Topouzelis N. The orthodontic-periodontic interrelationship in integrated treatment challenges: A systematic review. J Oral Rehabil, 2010, 37: 377–390
39 Gal J. About a synthetic saliva for *in vitro* studies. Talanta, 2001, 53: 1103–1115
40 Chen L, Hu W X, Du M, et al. Bioinspired, recyclable, stretchable hydrogel with boundary ultralubrication. ACS Appl Mater Interfaces, 2021, 13: 42240–42249
41 Qi X, Hu X, Wei W, et al. Investigation of Salecan/poly(vinyl alcohol) hydrogels prepared by freeze/thaw method. Carbohydrate Polyms, 2015, 118: 60–69
42 Costa-Júnior E S, Barbosa-Stancioli E F, Mansur A A P, et al. Preparation and characterization of chitosan/poly(vinyl alcohol) chemically crosslinked blends for biomedical applications. Carbohydr Polym, 2009, 76: 472—481
43 Fathi E, Atyabi N, Imani M, et al. Physically crosslinked polyvinyl alcohol-dextran blend xerogels: Morphology and thermal behavior. Carbohydrate Polyms, 2011, 84: 145–152
44 Qing X, He G, Liu Z, et al. Preparation and properties of polyvinyl alcohol/N-succinyl chitosan/lincomycin composite antibacterial hydrogels for wound dressing. Carbohydrate Polyms, 2021, 261: 117875
45 Durán-Guerrero J G, Martínez-Rodríguez M A, Garza-Navarro M A, et al. Magnetic nanofibrous materials based on CMC/PVA polymeric blends. Carbohydrate Polyms, 2018, 200: 289–296
46 Shadak Alee K, Kuladeep R, Narayana Rao D. *In-situ* investigation of the formation of silver nanoparticles in polyvinyl alcohol through micro-Raman spectroscopy. Optics Commun, 2013, 293: 69–74
47 El-Khodary A, Oraby A H, Abdelnaby M M. Characterization, electrical and magnetic properties of PVA films filled with $FeCl_3$-$MnCl_2$ mixed fillers. J Magn Magn Mater, 2008, 320: 1739–1746
48 Wang Q L, Zhu L, Wei D D, et al. Near-infrared responsive shape memory hydrogels with programmable and complex shape-morphing. Sci China Tech Sci, 2021, 64: 1752–1764
49 Chen Q, Zhu L, Chen H, et al. A novel design strategy for fully physically linked double network hydrogels with tough, fatigue resistant, and self-healing properties. Adv Funct Mater, 2015, 25: 1598–1607